Lipid-Anchored SNAREs Lacking Transmembrane Regions Fully Support Membrane Fusion during Neurotransmitter Release

Peng Zhou,[1,2] Taulant Bacaj,[1,2] Xiaofei Yang,[1,2,3] Zhiping P. Pang,[1,4] and Thomas C. Südhof[1,*]

[1]Department of Molecular and Cellular Physiology and Howard Hughes Medical Institute, Stanford University School of Medicine, 265 Campus Drive, Stanford, CA 94305, USA
[2]These authors contributed equally to this work
[3]Present address: South-Central University of the Nationalities, Wuhan, Hubei Province 430074, China
[4]Present address: Child Health Institute of New Jersey and Department of Neuroscience and Cell Biology, Rutgers-Robert Wood Johnson Medical School, New Brunswick, NJ 08901, USA
*Correspondence: tcs1@stanford.edu
http://dx.doi.org/10.1016/j.neuron.2013.09.010

SUMMARY

Synaptic vesicle fusion during neurotransmitter release is mediated by assembly of SNARE- and SM-protein complexes composed of syntaxin-1, SNAP-25, synaptobrevin-2/VAMP2, and Munc18-1. Current models suggest that SNARE-complex assembly catalyzes membrane fusion by pulling the transmembrane regions (TMRs) of SNARE proteins together, thus allowing their TMRs to form a fusion pore. These models are consistent with the requirement for TMRs in viral fusion proteins. However, the role of the SNARE TMRs in synaptic vesicle fusion has not yet been tested physiologically. Here, we examined whether synaptic SNAREs require TMRs for catalysis of synaptic vesicle fusion, which was monitored electrophysiologically at millisecond time resolution. Surprisingly, we find that both lipid-anchored syntaxin-1 and lipid-anchored synaptobrevin-2 lacking TMRs efficiently promoted spontaneous and Ca^{2+}-triggered membrane fusion. Our data suggest that SNARE proteins function during fusion primarily as force generators, consistent with the notion that forcing lipid membranes close together suffices to induce membrane fusion.

INTRODUCTION

Synaptic vesicle fusion and most other intracellular membrane fusion reactions are mediated by the concerted action of SNARE- and SM-proteins (reviewed in Rizo and Rosenmund, 2008; Sørensen, 2009; Südhof and Rothman, 2009). In presynaptic terminals, the R-SNARE protein synaptobrevin/VAMP on synaptic vesicles forms a tight complex with the Q-SNARE proteins syntaxin-1 and SNAP-25 on the plasma membrane, thereby forcing the synaptic vesicle and plasma membranes into proximity (Jahn et al., 2003). In addition, the SM protein

Munc18-1 binds to the SNARE complex throughout the assembly reaction (Dulubova et al., 2007; Shen et al., 2007) and is essential for fusion (Verhage et al., 2000; Khvotchev et al., 2007; Rathore et al., 2010; Zhou et al., 2013).

Multiple studies suggest that in addition to the SNARE motifs of synaptobrevin-2, syntaxin-1, and SNAP-25 that mediate SNARE-complex formation, the transmembrane regions (TMRs) of synaptobrevin-2 and syntaxin-1 are essential for membrane fusion and may induce fusion-pore opening (Han et al., 2004; Xu et al., 2005; Deák et al., 2006; Kesavan et al., 2007; Bretou et al., 2008; Lu et al., 2008; Stein et al., 2009; Fdez et al., 2010; Guzman et al., 2010; Ngatchou et al., 2010; Risselada et al., 2011; Shi et al., 2012). In yeast, replacement of the TMR of the synaptobrevin homolog Snc1p with a geranylgeranyl anchor not only blocked membrane fusion during exocytosis, but also even transformed Snc1p into an inhibitor of exocytosis (Grote et al., 2000). In PC12 cells, overexpression of syntaxin-1 altered the computed fusion-pore conductance during exocytosis dependent on the TMR sequence, suggesting that the TMRs line the fusion pore (Han et al., 2004). Moreover, partial deletion of the synaptobrevin-2 TMR blocked fusion (Fdez et al., 2010), and addition of residues to the C-terminal TMR of synaptobrevin-2 impeded fusion as well (Ngatchou et al., 2010).

At the molecular level, the TMRs of synaptobrevin-2 and syntaxin-1 interact with each other in vitro (Margittai et al., 1999; Laage et al., 2000). A crystal structure of the neuronal SNARE complex with attached TMRs revealed that the SNARE motifs and the TMRs of syntaxin-1 and synaptobrevin-2 form single continuously interacting α helices (Stein et al., 2009). This compelling result further supported the notion that the SNARE TMRs open the fusion pore, a model that was reinforced by liposome fusion experiments (Xu et al., 2005; Lu et al., 2008; Shi et al., 2012). Sophisticated computer simulations also indicated that SNARE TMRs initiate fusion by distorting the lipid packing of the outer membrane leaflets and by forming the fusion pore (Risselada et al., 2011). Moreover, increasing the distance of the SNARE complex from the TMR in synaptobrevin-2 impairs membrane fusion (Deák et al., 2006; Kesavan et al., 2007; Bretou et al., 2008; Guzman et al., 2010), corroborating the notion that SNARE-complex assembly needs to be tightly coupled to the

CrossMark

SNARE TMRs in order to promote fusion-pore formation by the TMRs.

Although at present the predominant model of SNARE-mediated fusion thus suggests that the SNARE TMRs play an essential role in fusion, not all experiments support such a model. Only one to three SNARE complexes are required for fusion (van den Bogaart et al., 2010; Mohrmann et al., 2010; Sinha et al., 2011), suggesting that the SNARE TMRs cannot form a ringed fusion pore. Moreover, although fusion of isolated yeast vacuoles is blocked by replacing the TMR of the R-SNARE Nyv1p (the synaptobrevin equivalent in this fusion reaction) with a lipid anchor, fusion can simply be restored by addition of excess Sec18p (the yeast NSF equivalent) and Vam7p (the SNAP-25 equivalent) (Jun et al., 2007). Similarly, liposomes containing reconstituted lipid-anchored Nyv1p fuse with proteoliposomes containing the cognate vacuolar Q-SNAREs after addition of excess HOPS complex (which contains the cognate SM protein Vps33 for this fusion reaction) and Sec17p and Sec18p (the SNAP and NSF equivalents), suggesting that in this in vitro fusion reaction the R-SNARE Nyv1p does not require a TMR (Xu et al., 2011). However, mutations of the TMR of Vam3p (the syntaxin-1 equivalent in yeast vacuole fusion) impaired membrane fusion of yeast vacuoles (Hofmann et al., 2006), arguing for a role of Q-SNARE TMRs in yeast vacuole fusion.

Given the predominant view that SNARE-mediated membrane fusion involves the SNARE TMRs analogous to viral fusion proteins that require a TMR (Kemble et al., 1994; Melikyan et al., 1995), it is surprising that the function of the SNARE TMRs has not been directly tested in a physiological fusion reaction, where fusion can be monitored in real time and with high sensitivity. Here, we have examined this question by measuring synaptic vesicle exocytosis in cultured neurons. We show that for both syntaxin-1 and synaptobrevin-2, replacement of the C-terminal TMR with a lipid anchor does not block the ability of these SNARE proteins to promote fusion, indicating that SNARE proteins without a TMR still promote fusion. Our data suggest that SNARE proteins may operate in membrane fusion simply by forcing lipid membranes close together without the need for a TMR-mediated transmembrane perturbation.

RESULTS

We used syntaxin-1-deficient cortical neurons that were cultured from syntaxin-1A KO mice and infected with either a control lentivirus or a syntaxin-1 knockdown (KD) lentivirus (Zhou et al., 2013). These neurons lack syntaxin-1A and exhibit a nearly complete loss of syntaxin-1B. They display a severe impairment in all forms of neurotransmitter release that can be rescued by re-expression of syntaxin-1A or syntaxin-1B, allowing syntaxin-1 structure/function analyses (Zhou et al., 2013). Because previous studies showed that inserting a short linker between the SNARE motif and the TMR of synaptobrevin-2 drastically impairs membrane fusion (Deák et al., 2006; Kesavan et al., 2007; Bretou et al., 2008; Guzman et al., 2010), we first tested whether syntaxin-1 exhibits the same coupling requirement between SNARE-complex assembly and the TMR as synaptobrevin-2.

We found that inserting only three or seven residues (approximately one or two α helix turns) into syntaxin-1A at a position

N-terminal to the TMR (Figure 1A, referred to as Syntaxin-1A^{3i} and as Syntaxin-1A^{7i}, respectively) did not decrease the function of syntaxin-1A in spontaneous mini release (Figures 1B and 1C; Figures S1A and S1B available online). However, these insertions blocked the ability of syntaxin-1A to rescue the impairment of release evoked by isolated action potentials or by action-potential trains in syntaxin-1 deficient neurons (Figures 1D–1F). Interestingly, the three- and seven-residue insertion mutants not only were unable to rescue the desynchronization of release in syntaxin-1 deficient neurons (measured as the SD of rise times and the coefficient of variation of this SD; Maximov and Südhof, 2005), but also strongly aggravated desynchronization of release (Figure 1E). Moreover, these insertion mutations blocked the ability of syntaxin-1A to rescue release evoked by hypertonic sucrose, which monitors the readily releasable pool (RRP) of synaptic vesicles (Rosenmund and Stevens, 1996; Figure 1G).

The finding that the three-residue insertion blocks release evoked by an action potential supports the notion that the precise coupling of SNARE-complex assembly to the TMRs drives fusion-pore opening via formation of a continuous α helix (Stein et al., 2009). However, the fact that spontaneous release is not impaired by the same insertion—as previously observed for synaptobrevin-2 (Deák et al., 2006), and reconfirmed in new experiments for the present study (Figure S2)—suggests alternative explanations. Clearly the three-residue insertion does not block fusion per se, and the coupling of the SNARE motif to the TMR thus is not essential for fusion as such, but only for the rapid synchronous Ca^{2+}-triggering of fusion.

We therefore asked whether the function of syntaxin-1 in fusion actually requires a TMR. In considering this question, we noted that the syntaxin-1 homologs syntaxin-11 and syntaxin-19 contain a palmitoyl-lipid anchor instead of a TMR, suggesting that a SNARE TMR may not be universally involved in fusion. We replaced the TMR of syntaxin-1A with the lipid anchor of syntaxin-19 without or with a seven-residue linker in case the precise distance of the SNARE motif from the membrane was important (Figure 2A, referred to as Syntaxin-1A$^{\Delta TMR}$ and as Syntaxin-1A$^{\Delta TMR+7i}$, respectively). We then examined the function of lipid-anchored syntaxin-1A in membrane fusion during synaptic vesicle exocytosis.

Strikingly, we found that lipid-anchored syntaxin-1A rescued the loss of spontaneous release at excitatory and inhibitory synapses in syntaxin-1-deficient neurons (Figures 2B, 2C, S3A, and S3B), as well as the impairment in evoked release in these neurons (Figures 2D–2G and S3C). Syntaxin-1A$^{\Delta TMR}$ partly reversed the decreased speed of release and fully rescued the desynchronization of release, whereas Syntaxin-1A$^{\Delta TMR+7i}$ completely rescued both (Figure 2E). Moreover, lipid-anchored syntaxin-1A without or with the seven-residue insertion was fully capable of maintaining sustained release evoked by a 10 Hz stimulus train (Figure 2F), and supported release induced by hypertonic sucrose as a measure of the RRP (Figure 2G). Thus, syntaxin-1A does not need a TMR for promoting synaptic membrane fusion.

It is puzzling that for wild-type syntaxin-1A containing a TMR, an insertion of as little as three residues between the SNARE motif and the TMR blocks fusion (Figure 1), whereas for lipid-anchored syntaxin-1A, the seven-residue insertion apparently
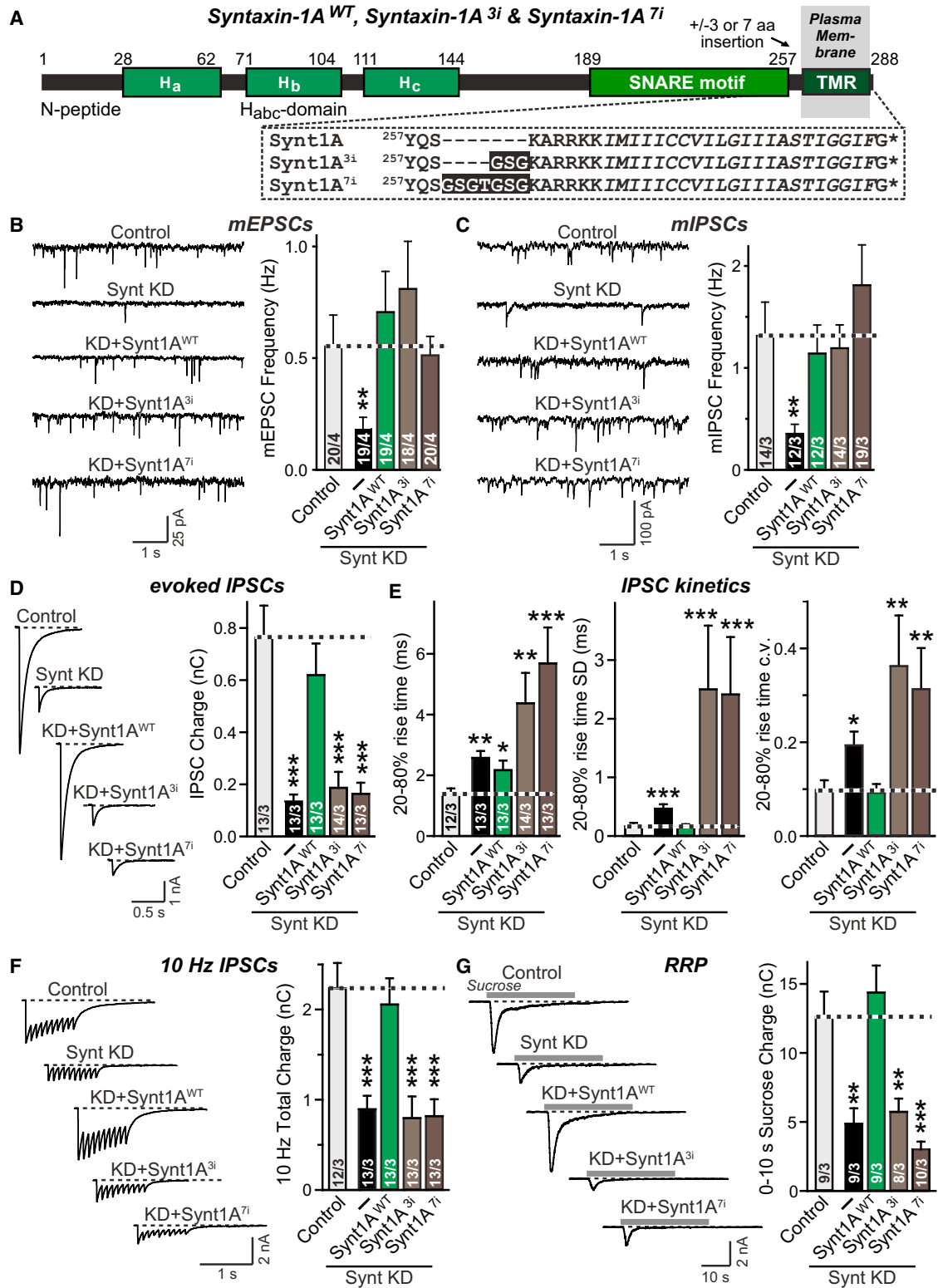
Figure 1. Tight Coupling of Syntaxin-1 SNARE Motif and TMR Is Essential for Ca^{2+}- and Hypertonic Sucrose-Triggered Synaptic Vesicle Fusion, but Not for Spontaneous Fusion

(A) Domain structure and C-terminal sequences of wild-type (Synt1A^{WT}) and mutant syntaxin-1A with three-residue (Synt1A^{3i}) or seven-residue (Synt1A^{7i}) insertions between the SNARE motif and TMR.

(legend continued on next page)

improved the fusogenic activity (Figure 2). This observation could be due to a difference in the fusion mechanism for TMR-versus lipid-anchored syntaxin-1A, so that the distance of the SNARE motif to the membrane anchor is functionally irrelevant for the latter. Alternatively, this finding could be due to a different optimal distance of the SNARE motif from the membrane anchor for TMR- and lipid-anchored syntaxin-1. To differentiate between these two possibilities and to test whether lipid-anchored and wild-type syntaxin-1A act by similar mechanisms, we examined the effect of further amino acid insertions between the SNARE motif and the lipid anchor in syntaxin-1A. In these experiments, we tested insertions of additional 3, 7, or 14 residues on top of the seven-residue insertion characterized above (referred to as Syntaxin-1A$^{\Delta TMR+10i}$, Syntaxin-1A$^{\Delta TMR+14i}$, and Syntaxin-1A$^{\Delta TMR+21i}$, respectively; Figure S4A).

We found that all insertion mutants of lipid-anchored syntaxin-1A rescued the impairment of spontaneous release in syntaxin-deficient neurons (Figures 3A and 3B). Unexpectedly, the longer insertions seemed to even increase mIPSCs, suggesting that they may "unclamp" spontaneous release. We detected no consistent change in the amplitudes and kinetics of spontaneous release under any condition (Figure S4B). When we examined action-potential-evoked release, however, we observed that similar to TMR-anchored syntaxin-1A, insertion of an additional three amino acids in lipid-anchored synaxin-1A on top of the seven-residue insertion (which by itself improved evoked release; Figure 2) blocked evoked release (Figure 3C). This phenotype was associated with a large increase in the desynchronization of release as measured via the variability of rise times (Figure 3D). Moreover, the additional insertions into lipid-anchored syntaxin-1A also blocked the ability of syntaxin-1A to rescue fusion induced by stimulus trains in syntaxin-deficient neurons (Figure 3E). Thus, lipid-anchored syntaxin-1A essential behaves like wild-type syntaxin-1A, with the same selective requirement for a precise distance between the SNARE motif and the membrane anchor for evoked but not for spontaneous release, except that the optimal distance of the SNARE motif from the membrane anchor appears to be slightly longer.

Most studies demonstrating an essential role for a SNARE TMR in fusion were performed with synaptobrevin-2. Is it possible that a TMR is only required in the R-SNARE synaptobrevin-2 instead of the Q-SNARE syntaxin-1, as also suggested by the presence of naturally occurring lipid-anchored syntaxins? To address this question, we searched for a strategy that would

allow us to attach the cytoplasmic synaptobrevin-2 sequences to the synaptic vesicle membrane by a lipid modification without a TMR.

However, this goal was difficult to achieve because most lipid-anchored synaptobrevin-2 mutants we tested were mistargeted. For example, geranyl-geranylated versions of synaptobrevin-2 carrying the C-terminal sequence of Rab3A were ineffective even though Rab3A itself is a synaptic vesicle protein (Johnston et al., 1991). Only when we fused the cytoplasmic synaptobrevin-2 sequence to the C-terminal palmitoylated sequence of cysteine-string protein-α (CSPα) did we observe good targeting of lipid-anchored synaptobrevin-2 to synapses (Figure 4). In these experiments, we compared two synaptobrevin-CSPα fusion proteins that differed by two residues (Figure 4A; referred to as Syb2$^{\Delta TMR\#1}$ and Syb2$^{\Delta TMR\#2}$), and employed neurons from synaptobrevin-2 KO mice to express these proteins in the complete absence of endogenous synaptobrevin-2 (Schoch et al., 2001).

Quantification of the levels and targeting of lipid-anchored synaptobrevin-2 revealed that the concentration of both synaptobrevin-CSPα fusion proteins represented ∼35%–45% of wild-type synaptobrevin-2 rescue protein (expressed as an mVenus fusion protein), and that they were targeted to synapses almost as effectively as wild-type synaptobrevin-2 (Figures 4B–4E). In these experiments, the longer version of lipid-anchored synaptobrevin-2 (Syb2$^{\Delta TMR\#2}$) containing two extra residues was expressed at slightly lower levels and was targeted to synapses with a lower efficiency than the shorter version (Syb2$^{\Delta TMR\#1}$).

In the next set of experiments, we tested the function of lipid-anchored synaptobrevin-2. We found that the shorter lipid-anchored synaptobrevin-2 (Syb2$^{\Delta TMR\#1}$) was as efficient as wild-type synaptobrevin-2 in rescuing spontaneous excitatory or inhibitory mini release in synaptobrevin-2 KO neurons, whereas the longer lipid-anchored synaptobrevin-2 (Syb2$^{\Delta TMR\#2}$) was less efficient (Figure 5). This rescue was observed for both the frequency and the amplitude of spontaneous events; the latter is decreased in synaptobrevin-2 KO neurons probably because of the role of synaptobrevin in AMPA-receptor exocytosis (Jurado et al., 2013). Strikingly, synaptobrevin-deficient neurons exhibited a significant increase in the rise times of mEPSCs and of mIPSCs, possibly because the remaining sporadic fusion events observed in these neurons are mediated by a noncognate SNARE protein (Figure 5; Schoch et al., 2001). This phenotype again was fully rescued by
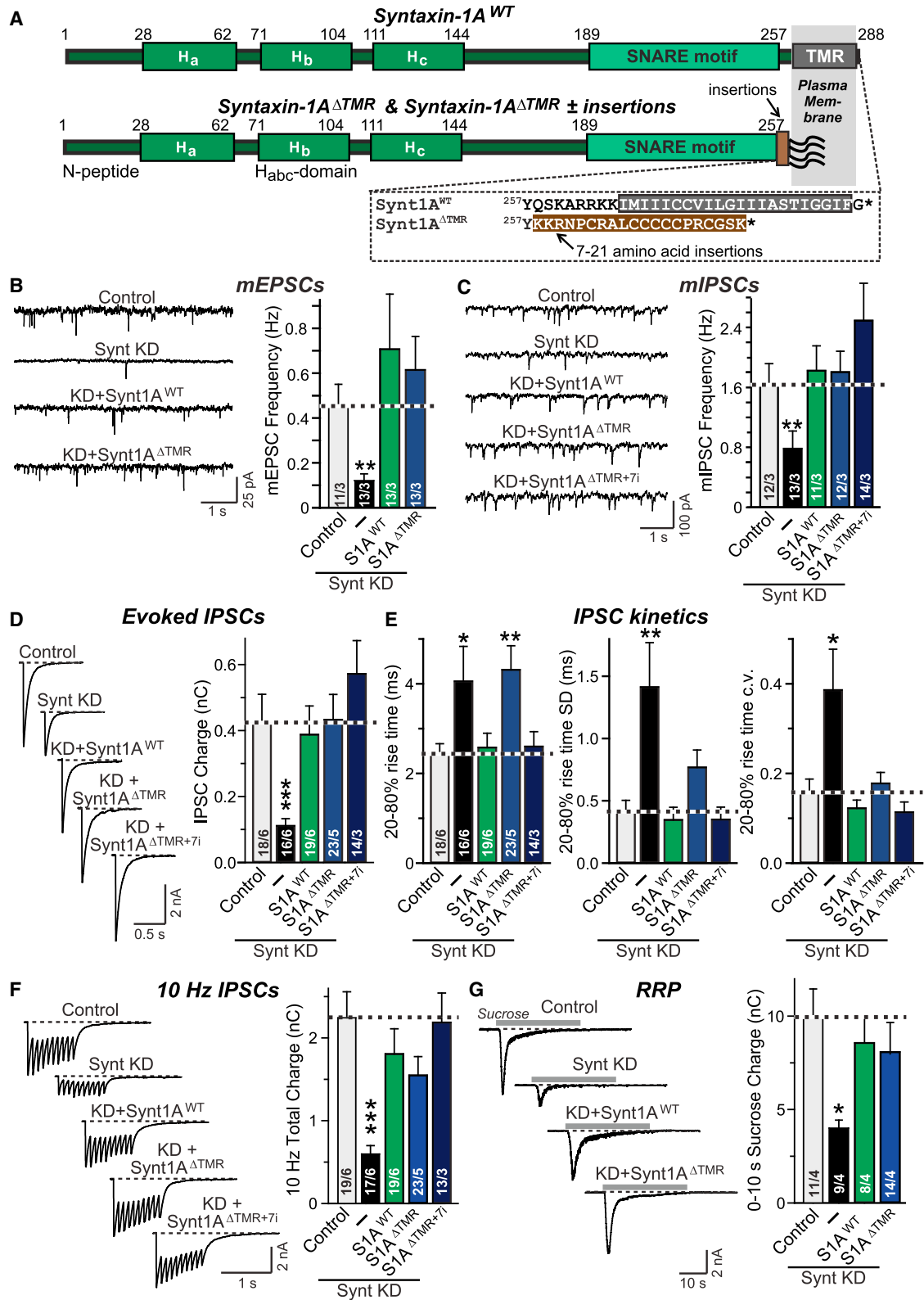
(B and C) Representative traces (left) and summary graphs of the frequency (right) of miniature excitatory (mEPSCs; B) and miniature inhibitory postsynaptic currents (mIPSCs; C) in cortical neurons cultured from syntaxin-1A KO mice and infected with control lentivirus (Control), or lentiviruses expressing only syntaxin-1 shRNAs (−), or syntaxin shRNAs together with shRNA-resistant wild-type (Synt1A^{WT}) or shRNA-resistant mutant syntaxin-1A with a three- (Synt1A^{3i}) or seven-residue insertion (Synt1A^{7i}). mEPSCs and mIPSCs were recorded in 1 μM TTX and either 50 μM picrotoxin (mEPSCs) or 10 μM CNQX and 50 μM AP-5 (mIPSCs).
(D) Representative traces (left) and summary graphs of the charge transfer (right) of inhibitory postsynaptic currents (IPSCs) evoked by isolated action potentials, monitored in cortical neurons as described for (C) but without TTX.
(E) Summary graphs of the IPSC rise times (left), and the variability of IPSC rise times expressed as the standard deviation (SD; middle) and the coefficient of variation (c.v.; right) of these rise times.
(F) Representative traces (left) and summary graphs of the total synaptic charge transfer (right) of IPSCs evoked by 10 stimuli applied at 10 Hz, monitored in cortical neurons as described for (D).
(G) Representative traces (left) and summary graphs of the total synaptic charge transfer (right) of IPSCs evoked by a 30 s application of 0.5 M hypertonic sucrose to induce exocytosis of the readily releasable pool of vesicles (RRP), monitored in cortical neurons as described for (B).
Data shown in summary graphs are means ± SEM; numbers of cells/independent cultures analyzed are listed in the bars. Statistical assessments were performed by Student's t test comparing each condition to the control (*p < 0.05; **p < 0.01; ***p < 0.001). For additional data, see Figures S1 and S2.

A Syntaxin-1A WT

Syntaxin-1A ΔTMR & Syntaxin-1A ΔTMR ± insertions

```
Synt1A^WT    ^257YQSKARRKK IMIIICCVILGIIIASTIGGIF G*
Synt1A^ΔTMR  ^257YKKRNPCRALCCCCCPRCGSK*
```
7-21 amino acid insertions

B mEPSCs

C mIPSCs

D Evoked IPSCs

E IPSC kinetics

F 10 Hz IPSCs

G RRP

(legend on next page)

lipid-anchored synaptobrevin-2, providing further evidence that lipid-anchored synaptobrevin-2 is functional.

Measurements of evoked release at different extracellular Ca^{2+}-concentrations demonstrated that lipid-anchored synaptobrevin-2 also rescued this fusion reaction, but was approximately half as efficient as wild-type synaptobrevin-2 (Figures 6A and S5). Moreover, both lipid-anchored synaptobrevin-2 versions rescued the desynchronization of release in synaptobrevin-2 KO neurons (Figure 6B). Finally, the lipid-anchored shorter version of synaptobrevin-2 was also able to partially rescue the decrease in the RRP present in synaptobrevin-2 KO neurons (Figure 6C). Overall, these experiments demonstrate that lipid-anchored synaptobrevin-2 is competent to promote SNARE-dependent synaptic vesicle fusion with an efficiency that correlates with its expression level and synaptic targeting.

Our data demonstrate that lipid-anchored syntaxin-1A and synaptobrevin-2 fully rescue the severely impaired spontaneous fusion in syntaxin- and synaptobrevin-deficient neurons, respectively, and additionally partially rescue impaired evoked fusion in these neurons. These data seem to suggest that the SNARE TMRs are not essential for fusion, and that only a lipid anchor is required. However, it is possible that the presence of only one of the two SNARE TMRs is sufficient for their proposed role in fusion-pore formation, although this notion is not consistent with models of the role of SNARE TMRs in fusion that are based on the interactions of these TMRs with each other (Stein et al., 2009). Thus, we examined whether the release phenotype of triple-deficient neurons lacking synaptobrevin-2, syntaxin-1A, and syntaxin-1B could be rescued by coexpressing lipid-anchored mutants of synaptobrevin-2 and syntaxin-1A.

We produced the triple-deficient neurons by generating double KO mice for syntaxin-1A and synaptobrevin-2, culturing neurons from these mice, and using the syntaxin-1 KD lentivirus to abrogate syntaxin-1B expression in these neurons. We then superinfected the synaptobrevin- and syntaxin-deficient neurons with a control lentivirus or with lentiviruses expressing either both wild-type syntaxin-1A and wild-type synaptobrevin-2, or both lipid-anchored syntaxin-1A and lipid-anchored synaptobrevin-2. Finally, we analyzed synaptic transmission in these three sets of neurons (Figures 7 and S6).

We found that lipid-anchored SNAREs were as effective as TMR-anchored wild-type SNAREs in rescuing spontaneous fusion in the synaptobrevin-2 and syntaxin-1A/B triple-deficient neurons (Figures 7A and 7B). This rescue included a reversal of the increased rise times of mini events observed in the triple-deficient neurons, suggesting that even when both fusing membranes contain lipid-anchored SNAREs, fusion-pore opening still proceeds with an apparently normal kinetics. Moreover, the lipid-anchored SNAREs rescued approximately 50% of release evoked either by isolated action potentials (Figure 7C), action potential trains (Figure 7D), or hypertonic sucrose (Figure 7E). However, although the rescue of evoked release was significant, lipid-anchored SNAREs were less efficient than TMR-anchored SNAREs in rescuing evoked release, consistent with a more important role of the coupling of SNARE complexes to the membrane anchor for evoked fusion than for spontaneous fusion.

DISCUSSION

How SNARE proteins promote membrane fusion remains a major question in cell biology. Using synaptic SNARE proteins, in vitro studies suggested that the SNARE TMRs may be central components of the fusion machinery (Han et al., 2004; Xu et al., 2005; Deák et al., 2006; Kesavan et al., 2007; Bretou et al., 2008; Lu et al., 2008; Stein et al., 2009; Fdez et al., 2010; Guzman et al., 2010; Ngatchou et al., 2010; Risselada et al., 2011; Shi et al., 2012). However, no direct test of this conclusion in a physiological context has been presented. Here, we demonstrate that the SNARE TMRs are unlikely to be essential for fusion since lipid-anchored syntaxin-1 and synaptobrevin-2 both were fully competent to support synaptic vesicle fusion in a physiological context. The lipid-anchored SNAREs completely rescued the impairment in spontaneous fusion in syntaxin- and synaptobrevin-deficient neurons, and partially rescued evoked release. Although lipid-anchored SNAREs were not as efficient as wild-type SNAREs in restoring the amplitude of evoked release in SNARE-deficient neurons, they reversed the impaired synchronization of evoked release, suggesting that impaired expression levels or incomplete targeting may in part account for the partial activity of lipid-anchored SNAREs in rescuing evoked release (Figure 4).

Figure 2. Syntaxin-1 TMR Is Not Essential for Synaptic Vesicle Fusion

(A) Domain structures of wild-type (top) and mutant syntaxin-1A in which the TMR replaced by a lipid-anchor sequence derived from syntaxin-19 (bottom; Synt1A$^{\Delta TMR}$) are shown. The sequences below the diagram depict the critical C-terminal region of wild-type and lipid-anchored syntaxin-1A. The position in lipid-anchored syntaxin-1A at which 7–21 amino acid insertions were placed is indicated by the arrow.

(B and C) Representative traces (left) and summary graphs of the frequency (right) of mEPSCs (B) and mIPSCs (C) in cortical neurons cultured from syntaxin-1A KO mice and infected with control lentivirus (Control), or lentiviruses expressing only syntaxin-1 shRNAs (−), or coexpressing the syntaxin shRNAs with wild-type syntaxin-1A (S1A^{WT}) or lipid-anchored syntaxin-1A without (S1A$^{\Delta TMR}$) or with a seven-residue insertion (S1A$^{\Delta TMR+7i}$).

(D) Representative traces (left) and summary graphs of the charge transfer (right) of IPSCs evoked by isolated action potentials, monitored in cortical neurons as described for (C).

(E) Summary graphs of the IPSC rise times (left), and variability of IPSC rise times expressed as the SD (middle) and the c.v. (right) of rise times as a measure of the desynchronization of release.

(F) Representative traces (left) and summary graphs of the total synaptic charge transfer (right) of IPSCs evoked by 10 stimuli applied at 10 Hz, monitored in cortical neurons as described for (C).

(G) Representative traces (left) and summary graphs of the total synaptic charge transfer (right) of IPSCs evoked by a 30 s application of 0.5 M hypertonic sucrose to induce exocytosis of the readily releasable pool of vesicles (RRP), monitored in cortical neurons as described for (B).

Data shown in summary graphs are means ± SEMs; numbers of cells/independent cultures analyzed are listed in the bars. Statistical assessments were performed by Student's t test comparing a condition to the control (*p < 0.05; **p < 0.01; ***p < 0.001). For additional data, see Figure S3.
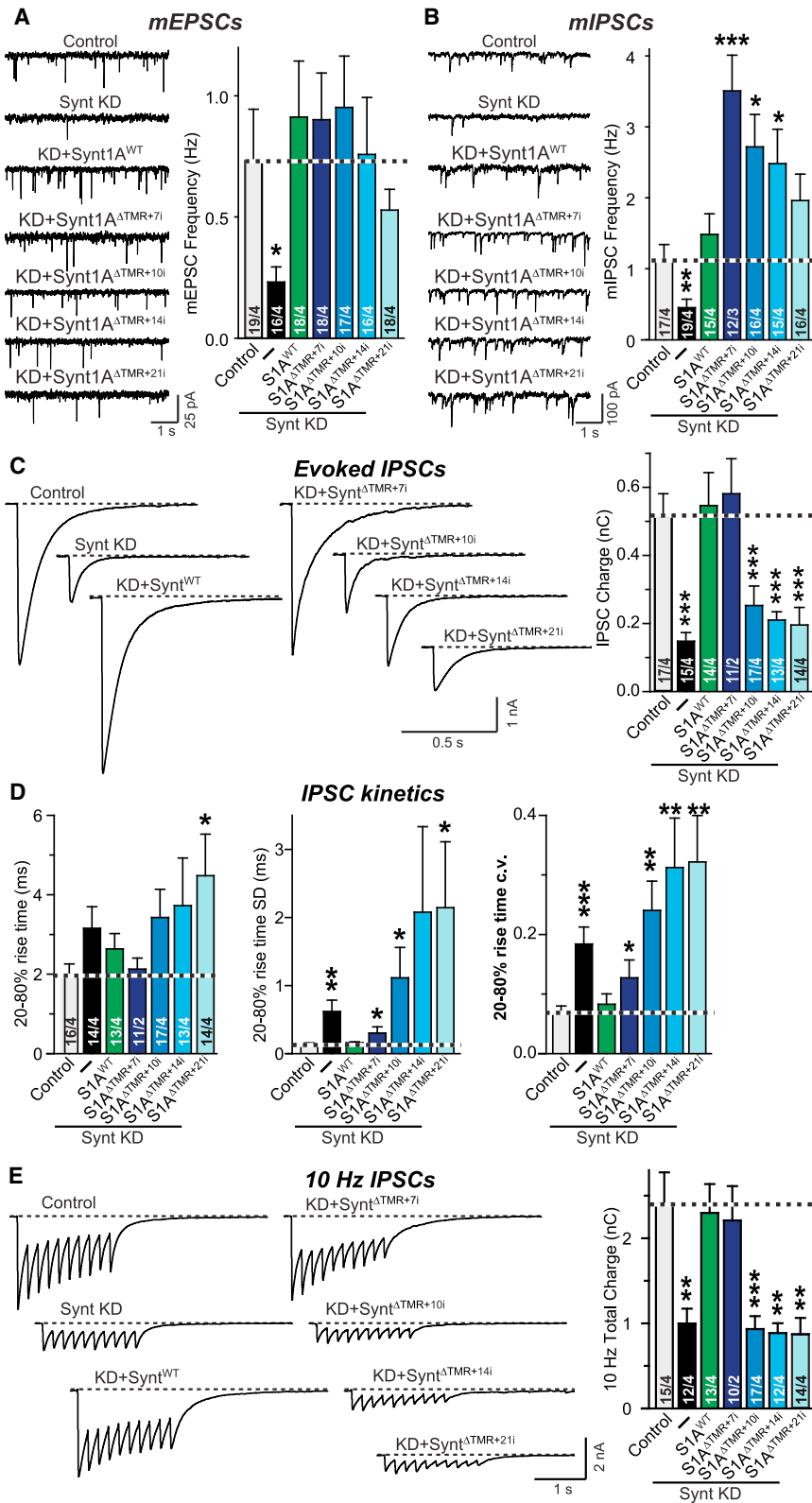
Figure 3. Tight Coupling of Syntaxin-1 SNARE Motif to the Lipid Anchor Is Essential for Evoked Synaptic Vesicle Fusion, but Not for Spontaneous Fusion

(A and B) Representative traces (left) and summary graphs of the frequency (right) of mEPSCs (A) and mIPSCs (B) in cortical neurons cultured from syntaxin-1A KO mice are shown. Neurons were infected with control lentivirus (Control), or lentiviruses expressing only syntaxin-1 shRNAs (−), or coexpressing syntaxin shRNAs together with shRNA-resistant wild-type (Synt1A^{WT}) or shRNA-resistant mutant syntaxin-1A with a lipid anchor instead of a TMR and insertions of 7 residues (Synt1A$^{\Delta TMR+7i}$), 10 residues (Synt1A$^{\Delta TMR+10i}$), 14 residues (Synt1A$^{\Delta TMR+14i}$), and 21 residues (Synt1A$^{\Delta TMR+21i}$). For insertion and flanking sequences, see Figures 2A and S4.

(C) Representative traces (left) and summary graphs of the charge transfer (right) of IPSCs evoked by isolated action potentials, monitored in cortical neurons as described for (A) and (B).

(D) Summary graphs of the IPSC rise times (left), and the variability of IPSC rise times expressed as the SD (middle) and the c.v. (right) of these rise times.

(E) Representative traces (left) and summary graphs of the total synaptic charge transfer (right) of IPSCs evoked by 10 stimuli applied at 10 Hz, monitored in cortical neurons as described for (A) and (B).

Data shown in summary graphs are means ± SEM; numbers of cells/independent cultures analyzed are listed in the bars. Statistical assessments were performed by Student's t test comparing each condition to control (*p < 0.05; **p < 0.01; ***p < 0.001).
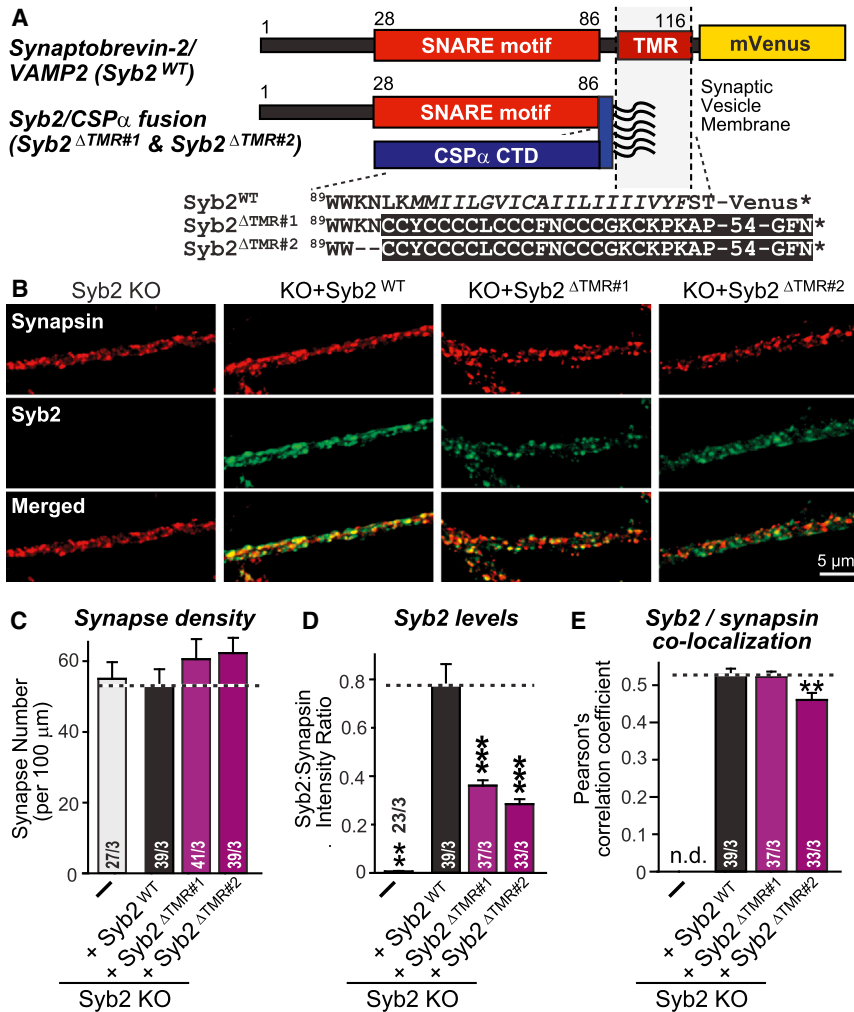
A

Synaptobrevin-2/
VAMP2 (Syb2 WT)

1	28	86	116	
	SNARE motif		TMR	mVenus

Syb2/CSPα fusion
(Syb2 ΔTMR#1 & Syb2 ΔTMR#2)

1	28	86	
	SNARE motif		Synaptic
	CSPα CTD		Vesicle Membrane

Syb2^WT   ⁸⁹WWKNLK*MMIILGVICAIILIIIIVYF*ST-Venus*
Syb2^ΔTMR#1   ⁸⁹WWKN**CCYCCCCLCCCFNCCCGKCKPKAP-54-GFN***
Syb2^ΔTMR#2   ⁸⁹WW--**CCYCCCCLCCCFNCCCGKCKPKAP-54-GFN***

B

Syb2 KO	KO+Syb2 WT	KO+Syb2 ΔTMR#1	KO+Syb2 ΔTMR#2
Synapsin			
Syb2			
Merged			

5 μm

C Synapse density

Synapse Number (per 100 μm)

27/3, 39/3, 41/3, 39/3

/ , + Syb2 WT, + Syb2 ΔTMR#1, + Syb2 ΔTMR#2

Syb2 KO

D Syb2 levels

Syb2:Synapsin Intensity Ratio

** 23/3, 39/3, *** 37/3, *** 33/3

/ , + Syb2 WT, + Syb2 ΔTMR#1, + Syb2 ΔTMR#2

Syb2 KO

E Syb2 / synapsin co-localization

Pearson's correlation coefficient

n.d., 39/3, 37/3, ** 33/3

/ , + Syb2 WT, + Syb2 ΔTMR#1, + Syb2 ΔTMR#2

Syb2 KO

Figure 4. Construction of Lipid-Anchored Synaptobrevin-2/VAMP2 that Is Still Targeted to Synapses

(A) Domain structures and C-terminal sequences of wild-type synaptobrevin-2 fused to mVenus (top; Syb2^WT), and mutant synaptobrevin-2 in which the TMR is replaced with the C-terminal region of CSPα (bottom), fused to synaptobrevin at either L93 (Syb2^ΔTMR#1) or K91 (Syb2^ΔTMR#2).

(B) Representative images of double immunofluorescence labeling for synapsin (red) and synaptobrevin-2 (green) in cortical neurons cultured from synaptobrevin-2 KO mice as described for Figure 4.

(C–E) Summary graphs of the synapse density (C), the levels of the various synaptobrevin-2 proteins (expressed as the intensity ratio between overlapped synaptobrevin-2 and synapsin immunoreactivity; D), and the colocalization of synaptobrevin-2 and synapsin (expressed as the Pearson's correlation coefficient; E) in images obtained as described for (A).

Data shown in summary graphs are means ± SEM; numbers of cells/independent cultures analyzed are listed in the bars. Statistical assessments were performed by Student's t test comparing a condition to the Syb KO + Syb^WT group (**p < 0.01; ***p < 0.001; n.d., nondetectable).

synaptobrevin-2 (Figures 4, 5, and 6) did not exclude the possibility that the SNARE TMRs still play a contributory role in fusion whereby only one of the two SNAREs (i.e., either syntaxin-1 or synaptobrevin) needs to be TMR anchored for fusion. However, the fact that spontaneous vesicle fusion in synaptobrevin- and syntaxin-double deficient neurons is fully rescued by reintroduction of lipid-anchored synaptobrevin-2 and synaxin-1A (Figures 7A and 7B) shows that fusion still proceeds even in the absence of any SNARE TMR and suggests that no SNARE TMR may be necessary for fusion per se. Moreover, the observation that evoked release is also significantly rescued in synaptobrevin- and syntaxin-triple deficient neurons by lipid-anchored SNAREs indicates that even for stimulated fusion, a SNARE TMR may not be absolutely necessary (Figures 7C–7E). We observed a small amount of remaining fusion in syntaxin- and synaptobrevin-deficient neurons that is probably mediated by the low levels of residual syntaxin-1B and by noncognate SNARE proteins present in these neurons, although we cannot exclude the possibility that an as-yet undiscovered non-SNARE fusion mechanism also contributes.

Alternative to our hypothesis that lipid-anchored SNARE proteins are fully fusion-competent and thus SNAREs do not form a proteinaceous fusion pore, it may be proposed that the low levels of residual syntaxin-1B and endogenous nonsynaptic SNARE proteins that mediate the residual fusion in syntaxin- and synaptobrevin-deficient neurons could collaborate with lipid-anchored rescue SNAREs in mediating fusion. This alternative hypothesis implies that each fusion reaction in SNARE-deficient
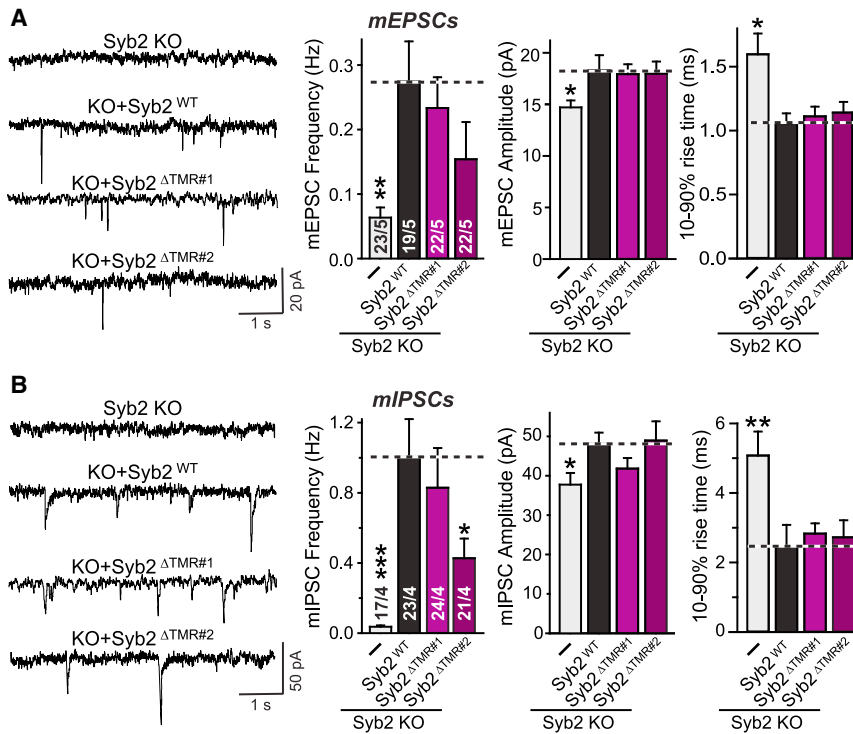
Our results suggest that a prevalent model whereby the SNARE TMRs are an essential component of the fusion machinery may need to be revised, and that SNAREs primarily—and maybe exclusively—operate as force generators for membrane fusion. According to this revised model, dehydrating the membrane surfaces of opposing membranes by forcing them closely together during SNARE-complex assembly may be sufficient to destabilize the phospholipid membrane surfaces and to induce fusion. Our data are consistent with the observation that protein-free liposomes form electrophysiologically "normal" fusion pores without protein components lining the pores (reviewed in Jahn et al., 2003) and argue against a necessary, direct role of SNARE TMRs in fusion-pore formation. It is tempting to speculate that the continued association of the SM protein Munc18-1 with SNARE complexes during all stages of fusion (Khvotchev et al., 2007; Rathore et al., 2010; Zhou et al., 2013) may reflect a contribution of Munc18-1 to the dehydration of the fusing membranes, thereby allowing spontaneous lipid mixing when SNARE-complex assembly forces membranes into close proximity, although no direct evidence supports this notion at present.

The experiments in which we tested the functionality of either lipid-anchored syntaxin-1 (Figures 2 and 3) or lipid-anchored

Figure 5. Lipid-Anchored Synaptobrevin-2 Fully Rescues Spontaneous Synaptic Vesicle Fusion in Synaptobrevin-2 KO Neurons

Representative traces (left) and summary graphs of the frequency (middle) and amplitude (right) of mEPSCs (A) and mIPSCs (B) in cortical neurons cultured from synaptobrevin-2 KO mice and infected with control lentivirus (−), or lentiviruses expressing either wild-type (Syb2^{WT}) or the two different versions of mutant lipid-anchored synaptobrevin-2 lacking the TMR (Syb2$^{\Delta TMR\#1}$ and Syb2$^{\Delta TMR\#2}$, respectively; see Figure 4). Data shown are means ± SEMs; numbers of cells/independent cultures analyzed are listed in the bars. Statistical assessments were performed by Student's t test comparing a condition to the wild-type rescue group (*p < 0.05; **p < 0.01; ***p < 0.001).

severely desynchronized, which suggests that this remaining fusion is qualitatively different from normal fusion, and that this desynchronization of fusion in SNARE-deficient neurons can be fully rescued with lipid-anchored SNAREs (Figures 2 and 6).

Our results do not imply that lipid-anchored SNAREs are as efficient as TMR-anchored SNAREs, and that the SNARE TMRs have no function. Quite the contrary, we show that lipid-anchored SNAREs are only as efficient as TMR-anchored SNAREs in fusion per se as evidenced by the complete rescue of spontaneous fusion with lipid-anchored SNARE proteins, but are not as efficient in evoked fusion (Figures 2, 3, 5, and 7). One of the functions of the SNARE TMRs may be to enable efficient targeting and recycling of SNARE proteins, as suggested by the incomplete targeting of lipid-anchored synaptobrevin-2 to synaptic vesicles (Figure 4).

In our experiments, we confirmed earlier results (Deák et al., 2006; Kesavan et al., 2007; Bretou et al., 2008; Guzman et al., 2010) that the tight coupling of the SNARE motif to the membrane anchor is particularly important for evoked fusion. The mechanistic difference we observe between spontaneous and evoked fusion is consistent with studies suggesting that spontaneous and evoked release are fundamentally different (Sara et al., 2005). The most parsimonious explanation for this part of our data is that fusion per se only requires a loose coupling of SNARE-complex assembly to membranes, but that evoked fusion requires a tight coupling of SNARE-complex assembly to membranes because evoked fusion operates on a partly preassembled, activated state that is then the substrate of the fusogenic stimulus (Südhof, 1995). The notion of such an activated state involving a tight coupling of SNARE-complex assembly to the membrane is also supported by the dramatic effects of mutations in juxtamembranous residues in synaptobrevin-2, which increase spontaneous fusion but impair evoked fusion (Maximov et al., 2009; Borisovska et al., 2012).
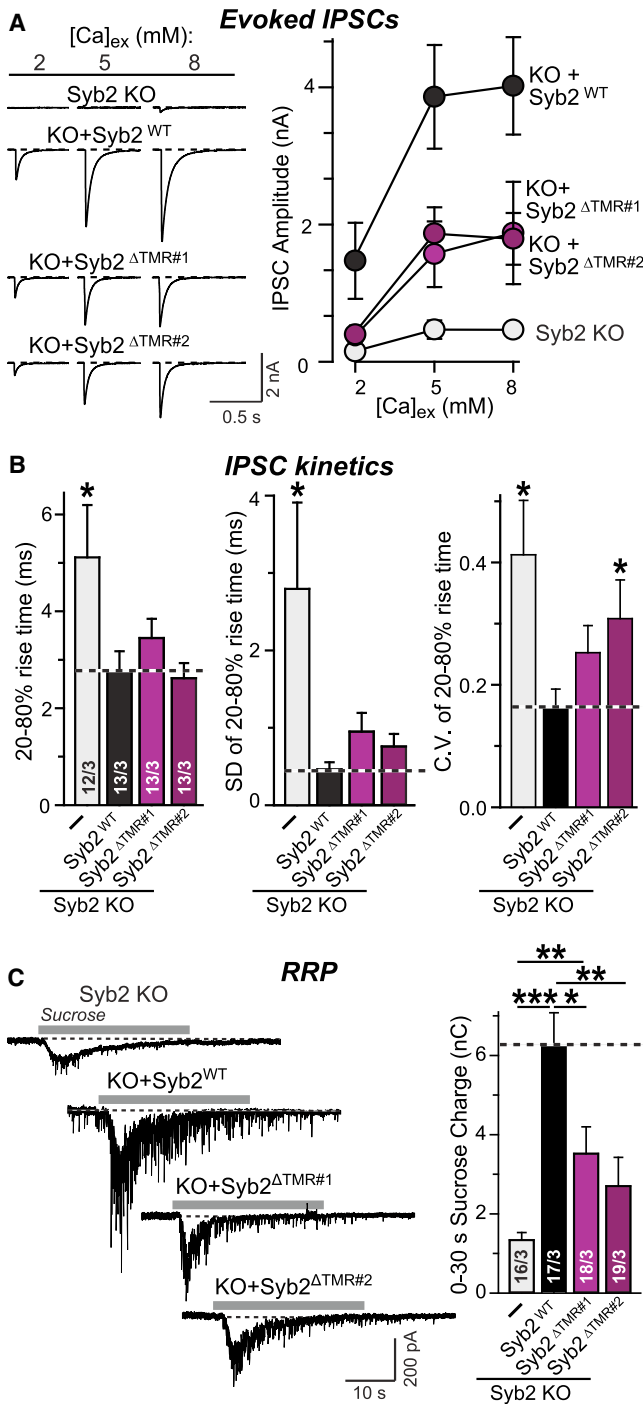
neurons rescued with lipid-anchored SNAREs is carried out by multiple SNARE complexes, of which at least one has to have a TMR but is nevertheless by itself unable to mediate fusion. According to this hypothesis, the major function of SNARE proteins still consists of mechanically forcing the fusing membranes together in order to account for the rescue phenotypes we observed (Figures 2, 3, 4, 5, 6, and 7), and the TMR would serve as a kind of "nucleus" for membrane perturbation and not as a proteinaceous fusion pore. Although we cannot completely rule out this hypothesis, we believe it is rather unlikely based on the following considerations.

The alternative hypothesis posits that (1) fusion must be mediated by many SNARE complexes because the nonsynaptic SNARE proteins alone cannot mediate full fusion; (2) all vesicles must contain such noncognate SNARE proteins; and (3) SNARE complexes in fusion are not equivalent. However, multiple studies have shown that fusion requires formation of only one to three SNARE complexes (van den Bogaart et al., 2010; Mohrmann et al., 2010; Sinha et al., 2011). Moreover, no noncognate SNARE protein that participates in synaptic vesicle fusion in addition to syntaxin-1, synaptobrevin, and SNAP-25 has been identified. Finally, it is difficult to envision a normal biological fusion mechanism in which SNARE complexes are not functionally equivalent. Thus, it seems to us more likely that only a small subset of vesicles contain noncanonical SNAREs which then account for the residual release observed in the syntaxin- or synaptobrevin-deficient neurons, and that a TMR is not required for fusion when lipid-anchored SNAREs rescue fusion. This conclusion would also account for the observation that the remaining fusion both in synaptobrevin-2 and in syntaxin-1 deficient neurons is

Why do our results appear to be diametrically opposite to at least some of the data in the literature (e.g, see Han et al., 2004; Xu et al., 2005; Kesavan et al., 2007; Bretou et al., 2008; Lu et al., 2008; Stein et al., 2009; Fdez et al., 2010; Guzman et al., 2010; Risselada et al., 2011; Shi et al., 2012)? Virtually all conclusions postulating an essential role of SNARE TMRs in fusion were based on overexpression experiments in non-neuronal cells or on reconstitution experiments with liposomes. In our view, overexpression experiments are unlikely to reveal what part of a SNARE protein is essential because all changes are induced by overexpression of a protein on the background of endogenous SNARE proteins. For example, elegant experiments in which wild-type and mutant syntaxin-1 was overexpressed in transfected PC12 cells revealed that mutations in the syntaxin-1 TMR altered fusion-pore properties in Ca^{2+}-stimulated exocytosis (Han et al., 2004). This result suggested the possibility that the syntaxin-1 TMR lines the fusion pore. However, overexpression of other proteins also leads to changes in fusion pore properties (e.g., see Fisher et al., 2001; Archer et al., 2002), suggesting that overexpressed proteins may affect the membrane tension in transfected cells, with the size of the effect dependent on the precise sequence of the protein and its expression levels, thereby accounting for the differences observed with mutations in the syntaxin-1 TMR.

With regard to the results from reconstitution experiments, it is striking that for neurotransmitter release in a real neuron, Munc18-1 is the single most important protein—the deletion of no other protein produces such a dramatic block of all fusion (Verhage et al., 2000). In reconstitution experiments, however, Munc18-1 is largely dispensable, although innovative new experiments have recently revealed major effects of Munc18-1 on liposome fusion (Shen et al., 2007; Rathore et al., 2010; Ma et al., 2013). It is therefore possible that the conditions of fusion in reconstitution experiments are still quite different from those operating physiologically, which may account for an essential role for TMRs during in vitro synaptic fusion reactions but not during physiological synaptic vesicle exocytosis.

SNARE-mediated membrane fusion is often modeled after fusion catalyzed by viral fusion proteins, such as influenza virus hemagglutinin. Classical studies revealed that hemagglutinin in which the TMR was replaced with a lipid anchor still efficiently induced hemifusion with outer membrane leaflet mixing, but blocked fusion-pore opening (Kemble et al., 1994; Melikyan et al., 1995). These results have led to the general notion that SNARE-mediated membrane fusion is mechanistically similar

---

Figure 6. Synaptobrevin-2 TMR Is Not Essential for Evoked Synaptic Vesicle Fusion

(A) Representative traces (left) and summary graphs of the amplitude (right) of IPSCs evoked by isolated action potentials, monitored in cortical neurons cultured from synaptobrevin-2 KO mice and infected with control lentivirus (−), or lentiviruses expressing either wild-type (Syb2^WT) or the two different versions of mutant lipid-anchored synaptobrevin-2 lacking the TMR (Syb2^ΔTMR#1 and Syb2^ΔTMR#2, respectively; see Figure 4). Recordings were carried out in bath solutions containing 2, 5, and 8 mM extracellular Ca^{2+} [Ca]_ex as indicated.

(B) Summary graphs of IPSC rise times (left), the variability of IPSC rise times (to assess the synchronicity of release; middle) expressed as the SD of rise times and the coefficient of variation of rise times (right) for IPSCs recorded in 5 mM [Ca^{2+}]_ex.

(C) Representative traces (left) and summary graphs of the total synaptic charge transfer (right) of IPSCs evoked by a 30 s application of 0.5 M hypertonic sucrose to induce exocytosis of the RRP, monitored in cortical neurons as described for (A).

Data shown in summary graphs are means ± SEMs; numbers of cells/independent cultures analyzed are listed in the bars. Statistical assessments were performed by Student's t test comparing a condition to the wild-type Syb2 rescue group (*p < 0.05; **p < 0.01; ***p < 0.001). See also Figure S5.
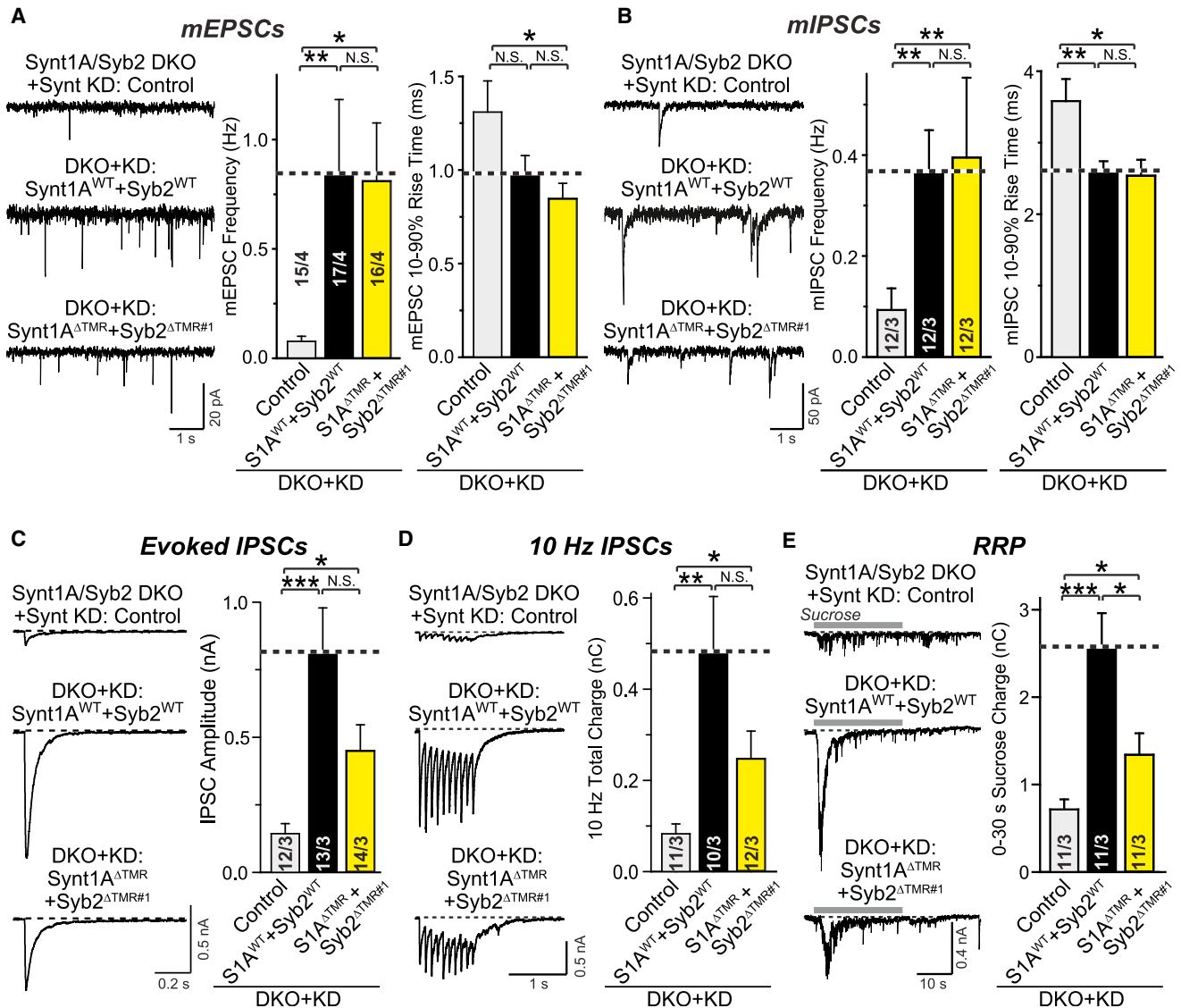
Figure 7. In Syntaxin/Synaptobrevin-Double-Deficient Neurons, Spontaneous Fusion Is Fully and Evoked Fusion Partially Rescued by Lipid-Anchored Syntaxin-1A and Synaptobrevin-2

(A and B) Representative traces (left) and summary graphs of the frequency (middle) and rise times (right) of mEPSCs (A) or mIPSCs (B) in cortical neurons cultured from syntaxin-1A/synaptobrevin-2 double KO mice and infected with lentiviruses expressing only syntaxin-1 shRNAs (Control), or coexpressing syntaxin shRNAs together with shRNA-resistant wild-type syntaxin-1A and wild-type synaptobrevin-2 (Synt1A^{WT}+Syb2^{WT}), or shRNA-resistant lipid-anchored syntaxin-1A and synaptobrevin-2 (Synt1A$^{\Delta TMR}$+ Syb2$^{\Delta TMR\#1}$).

(C) Representative traces (left) and summary graphs of the charge transfer (right) of IPSCs evoked by isolated action potentials, monitored in cortical neurons as described for (A) and (B).

(D) Representative traces (left) and summary graphs of the total synaptic charge transfer (right) of IPSCs evoked by 10 stimuli applied at 10 Hz, monitored in cortical neurons as described for (A) and (B).

(E) Representative traces (left) and summary graphs of the total synaptic charge transfer (right) of IPSCs evoked by a 30 s application of 0.5 M hypertonic sucrose to induce exocytosis of the RRP, monitored in cortical neurons as described for (A) and (B).

Data shown are means ± SEM; numbers of cells/independent cultures analyzed are listed in the bars. Statistical assessments were performed by Student's t test comparing each of the three conditions to each other (*p < 0.05; **p < 0.01; ***p < 0.001). See also Figure S6.

to viral membrane fusion (Söllner, 2004). Our results suggest that SNARE-mediated membrane fusion, however, is mechanistically different from viral membrane fusion, with the only shared property of the various fusion reactions being a need for dehydration of the membrane surface in order for fusion to

occur. The possibility of multiple mechanistically distinct fusion reactions in biology is consistent with the observation that homotypic fusion of mitochondria and of endoplasmic reticulum membranes may be mediated by dynamin-like GTPases with a different fusion mechanism (Wong et al., 2000; Hu et al.,

2009; Anwar et al., 2012). Moreover, myoblast fusion during development operates by yet another mechanism (Srinivas et al., 2007), suggesting that multiple independent membrane fusion mechanisms emerged during evolution. It thus seems plausible that some types of fusion, such as viral fusion mediated by a single fusion protein, require a TMR on one side of the membrane, whereas others, such as SNARE/SM protein mediated fusion mediated by a complex composed of four to five proteins, do not.

EXPERIMENTAL PROCEDURES

Neuronal Cultures

Neuronal cultures were obtained from mouse cortex as described (Yang et al., 2010). Briefly, mouse cortices were dissected from E18 of synaptobrevin-2 KO mice (Schoch et al., 2001) or postnatal day 1 (P1) of Syntaxin-1A KO mice (Gerber et al., 2008), dissociated by papain digestion (10 U/ml, with 1 μM Ca^{2+} and 0.5 μM EDTA) for 20 min at 37°C, plated on Matrigel-coated circular glass coverslips (12 mm diameter), and cultured in MEM (GIBCO) supplemented with 2% B27 (GIBCO), 0.5% w/v glucose, 100 mg/l transferrin, 5% fetal bovine serum, and 2 μM Ara-C (Sigma). Neurons were infected with lentiviruses at DIV5-7 and analyzed at DIV13-16. All animal procedures used were approved by Stanford institutional review boards.

Plasmid Construction

All experiments were performed with third-generation lentiviral vectors (L309S) that contained H1 and U6 pol III promoters, a human synapsin promoter, and an internal ribosome entry site (IRES) followed by GFP as described (Pang et al., 2010), and expressed two syntaxin-1 shRNAs (named ZP441; Zhou et al., 2013). Rescue experiments were performed with rat Syntaxin-1A rendered resistant to both shRNAs. To insert three or seven amino acids prior to the TMR, primers containing the desired junction sequence were used to first PCR-amplify the 3′ portion of the cDNA, then this "megaprimer" was used in conjunction with a 5′ primer to amplify the whole cDNA, which was inserted in ZP441 as an EcoRI fragment. The junction sequences encoded by these two constructs (named ZP449 and ZP450, respectively) are [257]YQS-GSG-KARRKKIMIIICCVILGIIIASTIGGIFG* and [257]YQS-GSGTGSG-KARRKKI MIIICCVILGIIIASTIGGIFG*. The Synt1A[ΔTMR] construct was made by PCR amplification of rat Syntaxin-1A cDNA with a primer that added the desired 3′ sequence, digested with EcoRI and inserted into ZP441. The junction region sequence was [257]Y-KKRNPCRALCCCCCPRCGSK (vector number ZP451).

For synaptobrevin-2 rescue experiments, the control vector (FSW-Venus) is the same as L309S but lacks the H1 and U6 promoters and expresses Venus instead of GFP. To make FSW-rSyb2-Venus (ZP456), a preexisting rat synaptobrevin-2 Venus fusion cDNA that contains the full-length cDNAs of each protein and a linker (RST), was cloned into the BamHI site of FSW as a BamHI/BglII fragment. To make the Syb2[ΔTMR#1] (ZP459) and Syb2[ΔTMR#2] (ZP460) constructs, a "megaprimer" consisting of the junction region and the CSPα sequence (amino acids 118–198) was amplified and was later used to PCR amplify from the rat synaptobrevin-2 cDNA; the junction regions initiate after synaptobrevin-2 amino acids 92 and 90, respectively. The PCR fragment was digested with XbaI/BamHI and was inserted into the XbaI/BamHI sites of FSW-Venus. The full sequence of the C terminus of CSPα is −CCYCCCCLCCCFNCCCGKCKPKAPEGEETEFYVSPEDLEAQLQ SDEREATDTPIVIQPASATETTQLTADSHPSYHTDGFN*.

Production of Lentiviruses

To make viruses, lentiviral expression vectors and three helper plasmids (pRSV-REV, pMDLg/pRRE, and pVSVG) were cotransfected into HEK293T cells (ATCC, VA), at 6, 2, 2, and 2 μg of DNA per 25 cm^2 culture area, respectively (Pang et al., 2010), using calcium phosphate, and cell-culture supernatants containing the viruses were collected 48 hr after transfection and directly used for infection of neurons. All steps were performed under level II biosafety conditions.

Immunocytochemistry

Neurons were fixed and permeabilized at −20°C in 100% methanol, incubated with antisynaptobrevin-2 (mouse monoclonal; CL69.1, Synaptic Systems) and antisynapsin (rabbit polyclonal; E028) primary antibodies in PBS with 4% BSA and 1% goat serum, washed, and stained with monoclonal antisynaptobrevin-2 and polyclonal antisynapsin and visualized using Alexa Fluor 633 goat antimouse and Alexa Fluor 546 goat antirabbit secondary antibodies (Molecular Probes). Images were acquired by using a Leica DMIRE2 confocal microscope equipped with a 63× oil-immersion objective with numerical aperture of 1.32. Identical settings were applied to all samples in each experiment. Stacks of z-section images were acquired and converted to maximal projection images by using Leica Confocal Software, and analyzed blindly with ImageJ 1.44p software (NIH, Bethesda). Images were thresholded by intensity to exclude the diffuse/intracellular pool, and then puncta were quantified by counting the number of suprathreshold areas of sizes between 0.25 and 4 μm^2. Pearson's correlation coefficients were calculated using ImageJ plugin of Mander's coefficients. Representative images were merged using ImageJ, with presynaptic terminals (visualized via synapsin staining) presented in red and synaptobrevin-2 in green.

Electrophysiological Recordings

Electrophysiological recordings were performed in whole-cell patch-clamp mode using concentric extracellular stimulation electrodes (Yang et al., 2010). Evoked synaptic responses were triggered by a bipolar electrode placed 100–150 μm from the soma of neurons recorded. Patch pipettes were pulled from borosilicate glass capillary tubes (Warner Instruments) using a PC-10 pipette puller (Narishige). The resistance of pipettes filled with intracellular solution varied between 3 and 5 MOhm. After formation of the whole-cell configuration and equilibration of the intracellular pipette solution, the series resistance was adjusted to 8–10 MOhm. Synaptic currents were monitored with a Multiclamp 700B amplifier (Molecular Devices). The frequency, duration, and magnitude of the extracellular stimulus were controlled with a Model 2100 Isolated Pulse Stimulator (A-M Systems) synchronized with Clampex 10 data acquisition software (Molecular Devices). The whole-cell pipette solution contained (120 mM CsCl, 5 mM NaCl, 1 mM $MgCl_2$, 10 mM HEPES, 10 mM EGTA, 0.3 mM Na-GTP, 3 mM Mg-ATP, and 5 mM QX-314 (pH 7.2, adjusted with CsOH). The bath solution contained 140 mM NaCl, 5 mM KCl, 2 mM $MgCl_2$, 2 mM $CaCl_2$, 10 mM HEPES, and 10 mM glucose (pH 7.4, adjusted with NaOH) except for the experiments in Figure 7 in which 5 mM $CaCl_2$ were included, and for the Ca^{2+}-titration experiments in Figure 6 in which the indicated concentrations of $CaCl_2$ were present. IPSCs and EPSCs were pharmacologically isolated by adding the AMPA and NMDA receptor blockers CNQX (10 μM) and AP-5 (50 μM) or the GABA$_A$-receptor blockers picrotoxin (50 μM) to the extracellular solution. Spontaneous mIPSCs and mEPSCs were monitored in the presence of tetrodotoxin (TTX; 1 μM) to block action potentials. Miniature events were analyzed in Clampfit 10 (Molecular Devices) using the template matching search and a minimal threshold of 5 pA and each event was visually inspected for inclusion or rejection by an experimenter blind to the recording condition. Sucrose-evoked release was triggered by a 30 s application of 0.5 M sucrose in the presence of AP-5, CNQX, and TTX, puffed by Picospritzer III (Parker).

Statistical Analyses

Statistical analyses were performed with Student's t tests comparing test to control samples analyzed in the same experiments.

REFERENCES

Anwar, K., Klemm, R.W., Condon, A., Severin, K.N., Zhang, M., Ghirlando, R., Hu, J., Rapoport, T.A., and Prinz, W.A. (2012). The dynamin-like GTPase Sey1p mediates homotypic ER fusion in *S. cerevisiae*. J. Cell Biol. *197*, 209–217.

Archer, D.A., Graham, M.E., and Burgoyne, R.D. (2002). Complexin regulates the closure of the fusion pore during regulated vesicle exocytosis. J. Biol. Chem. *277*, 18249–18252.

Borisovska, M., Schwarz, Y.N., Dhara, M., Yarzagaray, A., Hugo, S., Narzi, D., Siu, S.W., Kesavan, J., Mohrmann, R., Böckmann, R.A., and Bruns, D. (2012). Membrane-proximal tryptophans of synaptobrevin II stabilize priming of secretory vesicles. J. Neurosci. *32*, 15983–15997.

Bretou, M., Anne, C., and Darchen, F. (2008). A fast mode of membrane fusion dependent on tight SNARE zippering. J. Neurosci. *28*, 8470–8476.

Deák, F., Shin, O.H., Kavalali, E.T., and Südhof, T.C. (2006). Structural determinants of synaptobrevin 2 function in synaptic vesicle fusion. J. Neurosci. *26*, 6668–6676.

Dulubova, I., Khvotchev, M., Liu, S., Huryeva, I., Südhof, T.C., and Rizo, J. (2007). Munc18-1 binds directly to the neuronal SNARE complex. Proc. Natl. Acad. Sci. USA *104*, 2697–2702.

Fdez, E., Martínez-Salvador, M., Beard, M., Woodman, P., and Hilfiker, S. (2010). Transmembrane-domain determinants for SNARE-mediated membrane fusion. J. Cell Sci. *123*, 2473–2480.

Fisher, R.J., Pevsner, J., and Burgoyne, R.D. (2001). Control of fusion pore dynamics during exocytosis by Munc18. Science *291*, 875–878.

Gerber, S.H., Rah, J.C., Min, S.W., Liu, X., de Wit, H., Dulubova, I., Meyer, A.C., Rizo, J., Arancillo, M., Hammer, R.E., et al. (2008). Conformational switch of syntaxin-1 controls synaptic vesicle fusion. Science *321*, 1507–1510.

Grote, E., Baba, M., Ohsumi, Y., and Novick, P.J. (2000). Geranylgeranylated SNAREs are dominant inhibitors of membrane fusion. J. Cell Biol. *151*, 453–466.

Guzman, R.E., Schwarz, Y.N., Rettig, J., and Bruns, D. (2010). SNARE force synchronizes synaptic vesicle fusion and controls the kinetics of quantal synaptic transmission. J. Neurosci. *30*, 10272–10281.

Han, X., Wang, C.T., Bai, J., Chapman, E.R., and Jackson, M.B. (2004). Transmembrane segments of syntaxin line the fusion pore of Ca^{2+}-triggered exocytosis. Science *304*, 289–292.

Hofmann, M.W., Peplowska, K., Rohde, J., Poschner, B.C., Ungermann, C., and Langosch, D. (2006). Self-interaction of a SNARE transmembrane domain promotes the hemifusion-to-fusion transition. J. Mol. Biol. *364*, 1048–1060.

Hu, J., Shibata, Y., Zhu, P.P., Voss, C., Rismanchi, N., Prinz, W.A., Rapoport, T.A., and Blackstone, C. (2009). A class of dynamin-like GTPases involved in the generation of the tubular ER network. Cell *138*, 549–561.

Jahn, R., Lang, T., and Südhof, T.C. (2003). Membrane fusion. Cell *112*, 519–533.

Johnston, P.A., Archer, B.T., 3rd, Robinson, K., Mignery, G.A., Jahn, R., and Südhof, T.C. (1991). rab3A attachment to the synaptic vesicle membrane mediated by a conserved polyisoprenylated carboxy-terminal sequence. Neuron *7*, 101–109.

Jun, Y., Xu, H., Thorngren, N., and Wickner, W. (2007). Sec18p and Vam7p remodel trans-SNARE complexes to permit a lipid-anchored R-SNARE to support yeast vacuole fusion. EMBO J. *26*, 4935–4945.

Jurado, S., Goswami, D., Zhang, Y., Molina, A.J., Südhof, T.C., and Malenka, R.C. (2013). LTP requires a unique postsynaptic SNARE fusion machinery. Neuron *77*, 542–558.

Kemble, G.W., Danieli, T., and White, J.M. (1994). Lipid-anchored influenza hemagglutinin promotes hemifusion, not complete fusion. Cell *76*, 383–391.

Kesavan, J., Borisovska, M., and Bruns, D. (2007). v-SNARE actions during $Ca^{(2+)}$-triggered exocytosis. Cell *131*, 351–363.

Khvotchev, M., Dulubova, I., Sun, J., Dai, H., Rizo, J., and Südhof, T.C. (2007). Dual modes of Munc18-1/SNARE interactions are coupled by functionally critical binding to syntaxin-1 N terminus. J. Neurosci. *27*, 12147–12155.

Laage, R., Rohde, J., Brosig, B., and Langosch, D. (2000). A conserved membrane-spanning amino acid motif drives homomeric and supports heteromeric assembly of presynaptic SNARE proteins. J. Biol. Chem. *275*, 17481–17487.

Lu, X., Zhang, Y., and Shin, Y.K. (2008). Supramolecular SNARE assembly precedes hemifusion in SNARE-mediated membrane fusion. Nat. Struct. Mol. Biol. *15*, 700–706.

Ma, C., Su, L., Seven, A.B., Xu, Y., and Rizo, J. (2013). Reconstitution of the vital functions of Munc18 and Munc13 in neurotransmitter release. Science *339*, 421–425.

Margittai, M., Otto, H., and Jahn, R. (1999). A stable interaction between syntaxin 1a and synaptobrevin 2 mediated by their transmembrane domains. FEBS Lett. *446*, 40–44.

Maximov, A., and Südhof, T.C. (2005). Autonomous function of synaptotagmin 1 in triggering synchronous release independent of asynchronous release. Neuron *48*, 547–554.

Maximov, A., Tang, J., Yang, X., Pang, Z.P., and Südhof, T.C. (2009). Complexin controls the force transfer from SNARE complexes to membranes in fusion. Science *323*, 516–521.

Melikyan, G.B., White, J.M., and Cohen, F.S. (1995). GPI-anchored influenza hemagglutinin induces hemifusion to both red blood cell and planar bilayer membranes. J. Cell Biol. *131*, 679–691.

Mohrmann, R., de Wit, H., Verhage, M., Neher, E., and Sørensen, J.B. (2010). Fast vesicle fusion in living cells requires at least three SNARE complexes. Science *330*, 502–505.

Ngatchou, A.N., Kisler, K., Fang, Q., Walter, A.M., Zhao, Y., Bruns, D., Sørensen, J.B., and Lindau, M. (2010). Role of the synaptobrevin C terminus in fusion pore formation. Proc. Natl. Acad. Sci. USA *107*, 18463–18468.

Pang, Z.P., Xu, W., Cao, P., and Südhof, T.C. (2010). Calmodulin suppresses synaptotagmin-2 transcription in cortical neurons. J. Biol. Chem. *285*, 33930–33939.

Rathore, S.S., Bend, E.G., Yu, H., Hammarlund, M., Jorgensen, E.M., and Shen, J. (2010). Syntaxin N-terminal peptide motif is an initiation factor for the assembly of the SNARE-Sec1/Munc18 membrane fusion complex. Proc. Natl. Acad. Sci. USA *107*, 22399–22406.

Risselada, H.J., Kutzner, C., and Grubmüller, H. (2011). Caught in the act: visualization of SNARE-mediated fusion events in molecular detail. ChemBioChem *12*, 1049–1055.

Rizo, J., and Rosenmund, C. (2008). Synaptic vesicle fusion. Nat. Struct. Mol. Biol. *15*, 665–674.

Rosenmund, C., and Stevens, C.F. (1996). Definition of the readily releasable pool of vesicles at hippocampal synapses. Neuron *16*, 1197–1207.

Sara, Y., Virmani, T., Deák, F., Liu, X., and Kavalali, E.T. (2005). An isolated pool of vesicles recycles at rest and drives spontaneous neurotransmission. Neuron *45*, 563–573.

Schoch, S., Deák, F., Königstorfer, A., Mozhayeva, M., Sara, Y., Südhof, T.C., and Kavalali, E.T. (2001). SNARE function analyzed in synaptobrevin/VAMP knockout mice. Science *294*, 1117–1122.

Shen, J., Tareste, D.C., Paumet, F., Rothman, J.E., and Melia, T.J. (2007). Selective activation of cognate SNAREpins by Sec1/Munc18 proteins. Cell *128*, 183–195.

Shi, L., Shen, Q.T., Kiel, A., Wang, J., Wang, H.W., Melia, T.J., Rothman, J.E., and Pincet, F. (2012). SNARE proteins: one to fuse and three to keep the nascent fusion pore open. Science *335*, 1355–1359.

Sinha, R., Ahmed, S., Jahn, R., and Klingauf, J. (2011). Two synaptobrevin molecules are sufficient for vesicle fusion in central nervous system synapses. Proc. Natl. Acad. Sci. USA 108, 14318–14323.

Söllner, T.H. (2004). Intracellular and viral membrane fusion: a uniting mechanism. Curr. Opin. Cell Biol. 16, 429–435.

Sørensen, J.B. (2009). Conflicting views on the membrane fusion machinery and the fusion pore. Annu. Rev. Cell Dev. Biol. 25, 513–537.

Srinivas, B.P., Woo, J., Leong, W.Y., and Roy, S. (2007). A conserved molecular pathway mediates myoblast fusion in insects and vertebrates. Nat. Genet. 39, 781–786.

Stein, A., Weber, G., Wahl, M.C., and Jahn, R. (2009). Helical extension of the neuronal SNARE complex into the membrane. Nature 460, 525–528.

Südhof, T.C. (1995). The synaptic vesicle cycle: a cascade of protein-protein interactions. Nature 375, 645–653.

Südhof, T.C., and Rothman, J.E. (2009). Membrane fusion: grappling with SNARE and SM proteins. Science 323, 474–477.

van den Bogaart, G., Holt, M.G., Bunt, G., Riedel, D., Wouters, F.S., and Jahn, R. (2010). One SNARE complex is sufficient for membrane fusion. Nat. Struct. Mol. Biol. 17, 358–364.

Verhage, M., Maia, A.S., Plomp, J.J., Brussaard, A.B., Heeroma, J.H., Vermeer, H., Toonen, R.F., Hammer, R.E., van den Berg, T.K., Missler, M., et al. (2000). Synaptic assembly of the brain in the absence of neurotransmitter secretion. Science 287, 864–869.

Wong, E.D., Wagner, J.A., Gorsich, S.W., McCaffery, J.M., Shaw, J.M., and Nunnari, J. (2000). The dynamin-related GTPase, Mgm1p, is an intermembrane space protein required for maintenance of fusion competent mitochondria. J. Cell Biol. 151, 341–352.

Xu, Y., Zhang, F., Su, Z., McNew, J.A., and Shin, Y.K. (2005). Hemifusion in SNARE-mediated membrane fusion. Nat. Struct. Mol. Biol. 12, 417–422.

Xu, H., Zick, M., Wickner, W.T., and Jun, Y. (2011). A lipid-anchored SNARE supports membrane fusion. Proc. Natl. Acad. Sci. USA 108, 17325–17330.

Yang, X., Kaeser-Woo, Y.J., Pang, Z.P., Xu, W., and Südhof, T.C. (2010). Complexin clamps asynchronous release by blocking a secondary Ca^{2+} sensor via its accessory α helix. Neuron 68, 907–920.

Zhou, P., Pang, Z.P., Yang, X., Zhang, Y., Rosenmund, C., Bacaj, T., and Südhof, T.C. (2013). Syntaxin-1 N-peptide and H$_{abc}$-domain perform distinct essential functions in synaptic vesicle fusion. EMBO J. 32, 159–171.